Bioorganic & Medicinal Chemistry Letters 20 (2010) 2832–2836

Contents lists available at ScienceDirect

Bioorganic & Medicinal Chemistry Letters

journal homepage: www.elsevier.com/locate/bmcl

Imidazoacridin-6-ones as novel inhibitors of the quinone oxidoreductase NQO2

K. A. Nolan, M. P. Humphries, R. A. Bryce, I. J. Stratford *

School of Pharmacy and Pharmaceutical Sciences, the University of Manchester and Manchester Cancer Research Center, Oxford Road, Manchester M13 9PT, UK

ARTICLE INFO

Article history:
Received 18 February 2010
Revised 9 March 2010
Accepted 9 March 2010
Available online 15 March 2010

Keywords:
NQO2
Imidazoacridinones
Docking
Structure/activity relationships

ABSTRACT

The purpose of the work was to identify novel inhibitors of the enzyme NQO2. Using computational molecular modelling, a QSAR ($R^2 = 0.88$) was established, relating inhibitory potency with calculated binding affinity. From this, the imidazoacridin-6-one, **NSC660841**, was identified as the most potent inhibitor of NQO2 yet reported ($IC_{50} = 6$ nM).

© 2010 Elsevier Ltd. All rights reserved.

The oxidoreductases, NAD(P)H:quinone oxidoreductase 1 (NQO1, DT-diaphorase, EC 1.6.99.2) and NRH:quinone oxidoreductase 2 (NQO2, EC 1.10.99.2) are homodimeric, cytosolic flavoproteins that act as detoxifying enzymes. Their major physiological role is thought to be the ability to catalyse the two electron reduction of quinones to hydroquinones.[1,2] However, recently the two enzymes have been shown to demonstrate chaperone properties.[3–5] NQO1 has been shown to protect the tumour suppressor p53 against proteosomal degradation, leading to stabilization and activation of p53.[3,4] Further, inhibition of NQO1 enzyme activity leads to destabilization of p53.[3,4] Modulation of NQO2 activity can also have effects on p53 levels and function,[5] and in addition, deletion of NQO2 can alter intra-cellular signalling via the NF-κB pathway.[6,7]

We recently reported a virtual screening of the National Cancer Institute (NCI) chemical database in order to identify novel inhibitors of NQO1.[8,9] From this we identified the triazoleacridin-6-one, **NSC645827**, as a sub-micromolar inhibitor.[8] Subsequently we synthesized a series of compounds structurally related to **NSC645827** and identified efficient inhibitors of NQO1.[10] In addition, it was also established that some of these compounds were the most potent inhibitors of NQO2 yet reported.[10] We established a predictive QSAR model for these compounds, correlated computationally derived binding affinity with inhibitory potency and identified key molecular features which could confer the ability of compounds to inhibit NQO2.[10] On this basis we returned to the NCI chemical database to identify other putative inhibitors and from this analysis found a series of imidazoacridin-6-ones that showed excellent predicted binding characteristics to NQO2. Among these was **C1311** (**NSC645809**) a DNA binding agent[11–15] and inhibitor of FLT3 kinase,[16] that has undergone extensive clinical evaluation as an anti-cancer agent.[16,17] We obtained quantities of **C1311** from the NCI together with 16 closely related structural analogues (Table 1) and we report here their ability to inhibit the enzymatic activity of recombinant human NQO2. Using computational molecular modelling we established a reliable QSAR, and from this series of compounds, several are identified with inhibitory potencies (IC_{50}) of less than 10 nM. The compounds were further evaluated for cellular toxicity and their ability to bind to DNA.

Enzyme inhibitory potency was measured using recombinant human NQO2 (Sigma). This was diluted in 50 mM phosphate buffer to give an enzyme activity that would result in a change in optical absorbance of substrate of approximately 0.1 per minute. The enzyme reaction was started by adding 5 μL of this solution to 495 μL of 50 mM phosphate buffer at pH 7.4 containing 200 μM dihydronicotinamide riboside (NRH), together with 40 μM DCPIP (dichlorophenolindophenol) and various concentrations of the potential inhibitor dissolved in DMSO (final concentration 1.0% v/v). The DMSO concentration used is sufficiently small to ensure minimal perturbation of hydrogen bonding networks in aqueous NQO2 complexes. Reactions were carried out at 37 °C and reduction of DCPIP was monitored at 600 nm in a Beckman DU 650 spectrophotometer. IC_{50} values were determined using nonlinear curve fitting as implemented in the program Excel for which a 50% reduction of the initial rate was attained. Each measurement was made in triplicate and the experiments carried out three times. IC_{50} values, given in Table 1, are derived from each of these determinations. Examples of inhibition curves are given in Figure 2.

Values of IC_{50} for the imidazoacridin-6-ones cover two orders of magnitude. In order to gain insights into the structural basis for the differences in inhibitory potency, we computationally docked the compounds into the active site of NQO2 using the X-ray crystal

* Corresponding author. Tel.: +44 161 275 2487; fax: +44 161 275 8342.
E-mail address: ian.stratford@manchester.ac.uk (I.J. Stratford).

0960-894X/$ - see front matter © 2010 Elsevier Ltd. All rights reserved.
doi:10.1016/j.bmcl.2010.03.051

Table 1
Structures of the imidazoacridin-6-ones supplied by NCI (R-substituents as in Fig. 1), calculated (ΔG_{calcd}) and experimental (ΔG_{exp}) binding affinities; enzyme inhibitory potency (IC_{50}); toxicity toward HCT116 cancer cells, measured as the concentration required to reduce proliferation by 50% following a 96 h drug exposure; and ΔT_m, the change in melting temperature of calf thymus DNA exposured to 10 μM of each compound

NSC Number	R^1	n	R^2	R^3	R^4	R^5	R^6	ΔG_{calcd} kJ/mol	ΔG_{exp} kJ/mol	NQO2 inhibition IC_{50} (nM)	Toxicity HCT116 (μM)	ΔT_m (°C)
637991	Me	2	Me	H	H	OH	H	−50.3	−41.9	50 ± 1	0.65 ± 0.04	9.1 ± 0.2
637992	Et	2	Me	H	H	OH	H	−51.4	−44.8	16 ± 2	3.0 ± 0.64	8.6 ± 0.4
637993	Et	2	Me	H	H	OMe	H	−53.2	−46.2	9 ± 1	3.0 ± 0.98	8.6 ± 0.2
637994	Et	3	H	H	H	OH	H	−48.8	−35.8	597 ± 6	0.82 ± 0.11	8.0 ± 1.6
645808	Me	2	H	H	H	OH	H	−48.7	−37.5	296 ± 5	1.0 ± 0.81	5.1 ± 0.2
645809 (**C1311**)	Et	2	H	H	H	OH	H	−49.0	−39.2	148 ± 4	0.77 ± 0.15	4.5 ± 0.04
645811	Et	2	H	H	OH	H	H	−48.4	−34.6	953 ± 3	2.2 ± 0.19	5.0 ± 0.1
645812	Et	2	H	H	H	OMe	H	−47.8	−34.5	1000 ± 6	2.9 ± 0.75	4.5 ± 0.1
645831	Et	2	H	H	H	H	H	−48.8	−36.6	427 ± 25	1.0 ± 0.12	6.4 ± 0.5
645833	Me	2	H	H	H	H	H	−47.5	−34.9	830 ± 112	0.57 ± 0.06	5.6 ± 0.4
645834	Me	2	Me	H	H	H	H	−49.8	−37.3	323 ± 100	0.46 ± 0.06	7.1 ± 0.3
645835	Me	2	Et	H	H	H	H	−47.8	−35.4	693 ± 368	0.47 ± 0.02	5.1 ± 0.3
645836	Me	3	H	H	H	H	H	−49.9	−38.9	172 ± 19	0.86 ± 0.08	5.2 ± 0.3
660838	Et	2	H	OMe	H	H	H	−50.4	−40.2	99 ± 2	1.7 ± 0.92	5.0 ± 0.1
660839	Et	2	H	OMe	H	H	OMe	−52.8	−44.6	17 ± 3	1.67 ± 0.47	1.8 ± 0.7
660840	Et	2	H	OMe	H	H	OH	−52.4	−43.1	31 ± 2	0.54 ± 0.07	3.1 ± 0.7
660841	Et	2	H	H	OMe	OMe	OH	−52.8	−47.2	6 ± 3	0.95 ± 0.13	1.0 ± 0.3

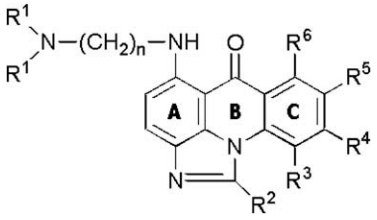

Figure 1. Structure of the imidazoacridine-6-ones obtained from NCI.

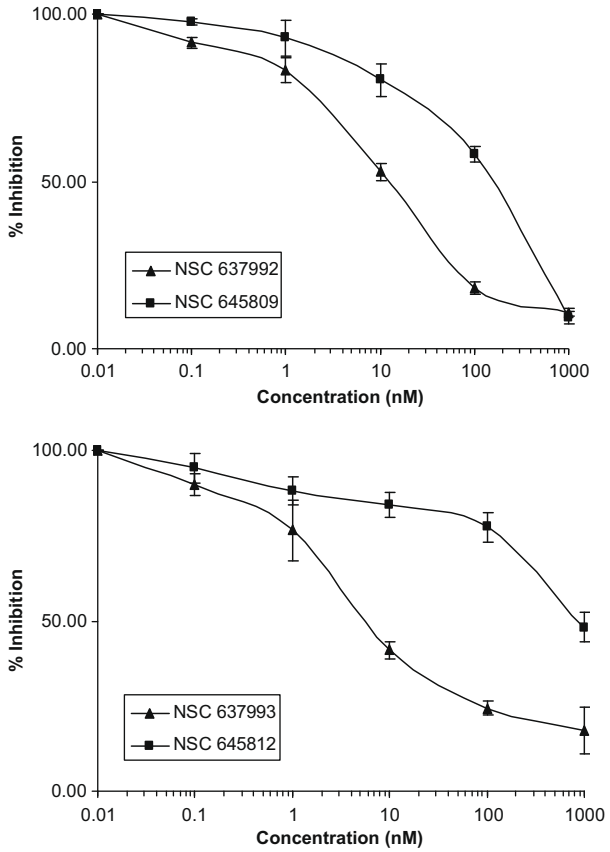

Figure 2. Inhibition of human recombined NQO2 by imidazoacridin-6-ones. Top panel, **NSC637992** (▲) and **NSC645809** (■); bottom panel, **NSC637993** (▲) and **NSC645812** (■). Each point is the mean (±SD) value derived from three independent experiments.

structure of human NQO2 with bound FAD (PDB code 1QR2, resolution at 2 Å). For docking purposes, the crystallographic coordinates of 1QR2 were obtained from the Brookhaven Database. Hydrogen atoms were added to the structure allowing for appropriate ionization at physiological pH. The FAD fragment was reatom typed to avoid underestimation by ChemScore of lipophilic/aromatic interactions.[18] The protonated complex was then minimized within SYBYL 7.3 (Tripos, St. Louis, USA 2009) whilst holding all heavy atoms stationary. Inspection of the active site showed a reasonable internal hydrogen bond network within the protein. Ligand structures were built and minimized with SYBYL 7.3. Flexible ligand docking was performed using the GOLD 4.1 software in combination with the ChemScore scoring function.[19] The top 20 solutions for each ligand were retained and analyzed for favourable interactions within the active site of NQO2. These included low protein–ligand clashes, ligand distortion energies, lipophilic contacts and hydrogen bonding interactions. After docking, the calculated binding affinities and experimental binding affinities, derived from IC_{50} values,[20] were compared (Table 1). An excellent correlation coefficient of $R^2 = 0.88$ (Fig. 3) was determined suggesting a reliable and predictive QSAR model for this series of structurally similar imidazoacridin-6-ones.

The docking calculations predicted only one energetically favourable binding mode for the imidazoacridin-6-ones. Most ligands are positioned in the centre of the active site and form π–π stacking interactions with the isoalloxazine ring of FAD, Trp105 and Phe178 (Fig. 4). Ligands also make good hydrophobic interactions with active site residues (Phe106, Phe126 and Ile128) and this is reflected in the lipophilic contribution to the docking scores. All ligands in this series form an internal hydrogen bond between the N5 proton and the ketone oxygen at C6 (2.0 Å); this limits rotation of the N5 side chain and holds the scaffold in a planar conformation (Fig. 4).

Replacing the methyl substituent at R^1 with an ethyl group causes a 2–3-fold increase (Table 1) in the potency of the compounds (compare **637991** and **637992**, **645808** and **645809**, **645833** and **645831**). Addition of a methyl substituent at R^2 in **637991**, **637992**, **637993** and **645834** causes the acridine scaffold to rotate with respect to the isoalloxazine ring of FAD and is well tolerated within the active site of NQO2 allowing additional hydrophobic interactions with Trp105 (Fig. 4A and C). The hydroxy group

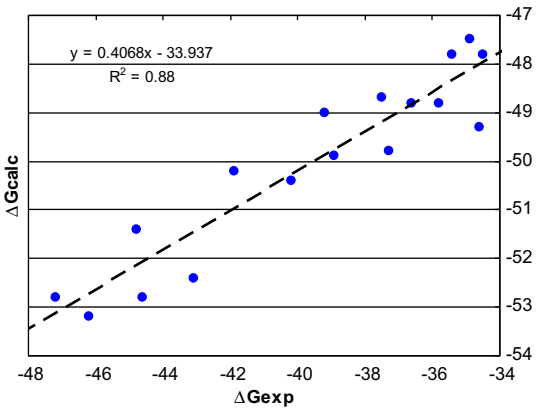

Figure 3. Experimental (ΔG_{exp}/kJ mol^{-1}) and calculated (ΔG_{calcd}/kJ mol^{-1}) affinities for the imidazoacridine-6-ones binding to NQO2. ΔG_{exp} is calculated from IC_{50} values using the Cheng–Prusoff equation.[20]

at R_5 on **637991** and **637992** (Fig. 4A) forms a hydrogen bond contact with Gln122. In contrast, **637994**, **645808** and **645809** (Fig. 4B) form a close hydrogen bond contact with Thr71 and this appears to influence the orientation of the ligand within the active site of the enzyme pulling it deeper into the binding pocket. The additional CH_2 group on the N5 side chain of **637994** causes steric hindrance with Ile128 and results in a fourfold decrease in potency from 148 nM for **645809** to 597 nM for **637994**. Interestingly, the QSAR model suggests that **645811** should be somewhat more potent than 953 nM since the hydroxy group at R^4 also makes a close hydrogen bond contact with Thr71.

The weakest inhibitor in this series of structurally related analogues is **645812** (Fig. 4D) with an IC_{50} of 1 μM. This compound has a methoxy substituent at R^5 (Fig. 1) which, in the absence of a methyl group at R^2 (**637993**), appears to move the acridine scaffold from the centre of the active site thus disrupting the π–π stacking interactions with the isoalloxazine ring of FAD and Phe178. Similarly, **645835** with an IC_{50} of 693 nM has an ethyl substituent at R^2 which causes rotation of the acridine scaffold as a consequence of steric clashes with Trp105 and Phe126. However, the docking studies suggest that multiple substitutions around the **C** ring at positions R^3, R^4, R^5 and R^6 (Fig. 1) are clearly well tolerated when R^2 contains a proton and this is clearly evident in Figure 5. For example, compounds **660839** and **660840** have IC_{50} values of 17 nM and 31 nM, respectively. Furthermore, the most potent inhibitor of NQO2 identified to date, is **660841** with an

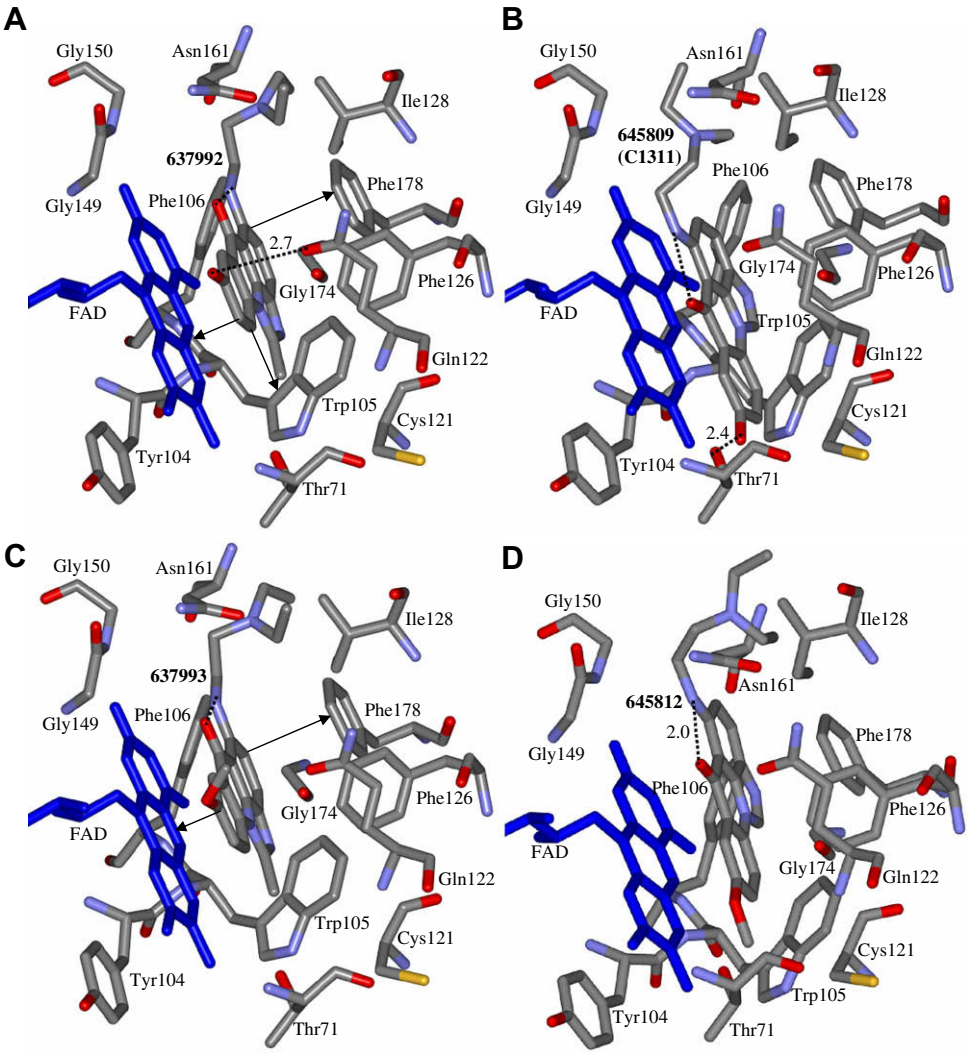

Figure 4. Compounds (A) **637992**, (B) **645809** (**C1311**), (C) **637993**, (D) **645812** docked in the active site of NQO2. FAD is coloured blue. Polar contacts are shown as dashed lines and π–π stacking interactions are shown as solid arrows in A and C. Distances are shown in Å.

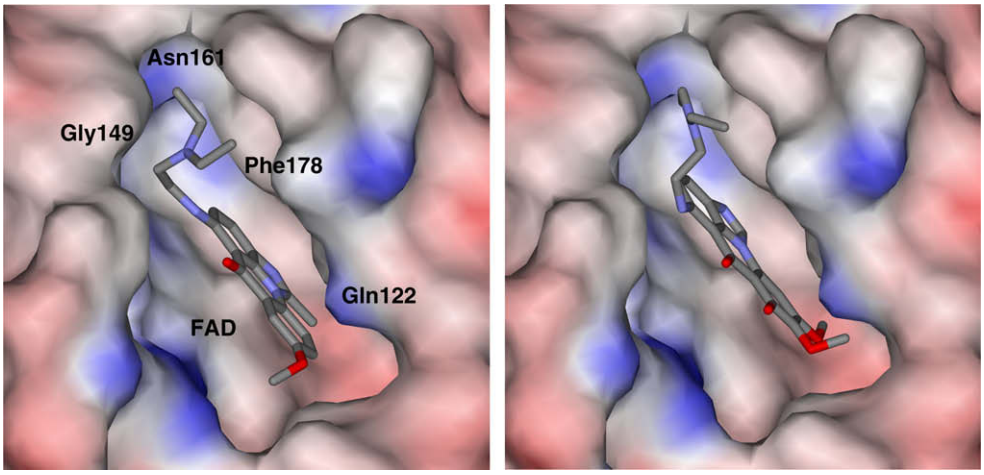

Figure 5. Electrostatic surface representations of NQO2 with **637993** (left panel) and **660841** (right panel) in the binding pocket. Several active site residues have been labeled in the left panel to compare with Figure 4C.

IC_{50} value of 6 nM. Figure 5 shows the orientation of the two most potent inhibitors, **637993** and **660841**, within the binding pocket of NQO2. By reference to Figure 4C (**637993**) the orientation of the molecule in the binding pocket can be compared, and this allows the key residue interactions to be related to the surface representation. Comparison of **637993** and **660841** in the binding pocket shows that the acridine scaffold rotates as a consequence of substitution in the imidazole (R^2) or in the **C** ring (R^3, R^4, R^5 and R^6). This results in the molecules being drawn into the hydrophobic cleft.

In order to determine the potential pharmacological usefulness of these compounds for inhibiting NQO2, we first measured the toxicity of the imidazoacridin-6-ones in HCT116 colon cancer cells. These cells show significant activity of NQO2 (493 ± 74 nmol DCPIP reduced/min/mg protein).[10] The cells were routinely maintained in monolayer in RPMI 1640, supplemented with 10% FCS (foetal calf serum) and 2 mM L-glutamine and toxicity was determined by the MTT assay as described previously.[21] Drug exposures were for 96 h. Values indicating the toxicity of each compound are given in Table 1 and represent the drug concentrations required to reduce proliferation by 50% relative to untreated and/or vehicle only treated cells. All experiments were carried out on at least three independent occasions. For this series of compounds values of toxicity cover a sixfold range and there appears to be no obvious relationship between toxicity and inhibitory potency towards NQO2. Thus, it is unlikely that enzyme inhibition is a major contributory factor to the toxicity of these compounds. As has been demonstrated by others[13–15] the imidazoacridin-6-ones have the ability to interact with DNA; we therefore evaluated the effects of the compounds on the melting temperature (T_m) of DNA. Calf thymus DNA (20 μg/ml) was treated with 10 μM of each compound in 7.5 mM NaH_2PO_4 and 1 mM EDTA at pH 7.0. Mixtures were heated from 37 to 98 °C and optical densities were measured at 260 nm at every °C. Values of T_m were determined from the mid-point of the hypochromic transition curves. In Table 1 values of ΔT_m are given; these are the differences in T_m of drug treated versus control DNA. As a positive control for changes in T_m we used adriamycin and under these conditions a ΔT_m value of 14.5 ± 0.9 °C was obtained. Inspection of the values in Table 1 indicates no relationship between T_m and toxicity. Interestingly, a methyl substituent at R^2 tends to give the higher values of ΔT_m, whereas greater substitution around the **C** ring (R^{3-6}, **660839**, **660840** and **660841**) gives the lowest values of ΔT_m. The most potent inhibitor of NQO2 (**660841**) has the lowest ΔT_m, which could provide direction for the subsequent design of NQO2 inhibitors.

Following the initial synthesis and evaluation of imidazoacridin-6-ones as anti-cancer agents by Konopa and co-workers,[11,12,22,23] there has been a substantial effort to establish their precise mechanism of action in vitro and in vivo.[13–15,24,25] This has been particularly important for **C1311** in order to help optimize its clinical application. The work reported here indicates that **C1311** can inhibit NQO2. Therefore, this property could contribute to its activity as has recently been suggested for the kinase inhibitor, imatinib.[26,27] However, the purpose of the current work was not to establish the mechanism by which **C1311** and the other imidazoacridin-6-ones kill cells, but rather to establish their ability (or lack of it) to inhibit the enzyme NQO2. In the literature, resveratrol is used as the standard inhibitor of NQO2 and using the enzyme assay reported here, the IC_{50} for resveratrol is 450 ± 150 nM.[10] In the present work, we have identified compounds that are active at concentrations <10 nM, which makes them the most potent inhibitors of NQO2 yet reported. It is known that genetic disruption of NQO2 function in cells and tissues can have profound effects on a variety of signalling functions in cells.[5–7,28] The compounds reported here together with a series of structurally similar triazoloacridin-6-ones[10] give leads for future development of agents that can provide a pharmacological means of modulating NQO2 function in vitro and in vivo.

Acknowledgements

This work was supported by an MRC programme grant to I.J.S. (G0500366) and a project grant from AICR (I.J.S., R.B. and K.A.N.). We thank the Drug Synthesis and Chemistry Branch, Developmental Therapeutics Program, Division of Cancer Treatment and Diagnosis, NCI, for the supply of the imidazoacridin-6-ones used in this work. Professor Nicola Tirelli is thanked for providing the facilities to carry out the DNA binding analysis. Dr. Roger Whitehead and Mr. John Barnes are thanked for providing the NRH.

References and notes

1. Ernster, L.; Navazio, F. *Biochem. Biophys. Acta* **1957**, *26*, 408.
2. Liao, S.; Williams-Ashman, H. G. *Biochem. Biophys. Res. Commun.* **1961**, *4*, 208.
3. Asher, G.; Bercovich, A.; Tsvetkov, P.; Shaul, Y.; Kahana, C. *Mol. Cell.* **2005**, *17*, 645.
4. Asher, G.; Tsvetkov, P.; Kahana, C.; Shaul, Y. *Gene Dev.* **2005**, *19*, 316.
5. Gong, X.; Kole, L.; Iskander, K.; Jaiswal, A. K. *Cancer Res.* **2007**, *67*, 5380.
6. Iskander, K.; Li, J.; Han, S.; Zheng, B.; Jaiswal, A. K. *J. Biol. Chem.* **2006**, *41*, 30917.
7. Ahn, K. S.; Gong, X.; Sethi, G.; Chaturvedi, M. M.; Jaiswal, A. K.; Aggarwal, B. B. *Cancer Res.* **2007**, *67*, 10004.
8. Nolan, K. A.; Timson, D. J.; Stratford, I. J.; Bryce, R. A. *Bioorg. Med. Chem. Lett.* **2006**, *16*, 6246.

9. Nolan, K. A.; Zhao, H.; Faulder, P. F.; Frenkel, A. D.; Timson, D. J.; Siegel, D.; Ross, D., ; Burke, T. R., Jr.; Stratford, I. J.; Bryce, R. A. *J. Med. Chem.* **2007**, *50*, 6316.
10. Nolan, K. A.; Humphries, M. P.; Barnes, J.; Doncaster, J. R.; Caraher, M. C.; Tirelli, N.; Bryce, R. A.; Whitehead, R. C.; Stratford, I. J. *Bioorg. Med. Chem.* **2010**, *18*, 696.
11. Cholody, W. M.; Martelli, S.; Paradziej-Lukowicz, J.; Konopa, J. *J. Med. Chem.* **1990**, *33*, 49.
12. Cholody, W. M.; Martelli, S.; Konopa, J. *J. Med. Chem.* **1992**, *35*, 378.
13. Skladanowski, A.; Plisov, S. Y.; Konopa, J.; Larsen, A. K. *Mol. Pharmacol.* **1996**, *49*, 772.
14. Burger, A. M.; Double, J. A.; Konopa, J.; Bibby, M. C. *Br. J. Cancer* **1996**, *74*, 1369.
15. Dziegielewski, J.; Slusarski, B.; Konitz, A.; Skladanowski, A.; Konopa, A. *J. Biochem. Pharmacol.* **2002**, *63*, 1653.
16. Thomas, A. L.; Anthoney, A.; Scott, E.; Ahmed, S.; Lundberg, A. S.; Major, A.; Capizzi, R. L.; Twelves, C. J. Abstract of Papers, 44th Annual MeetingAmerican Society of Clinical Oncology, Chicago, Illinois, ASCO Proceedings, *J. Clin. Oncol.* **2008**; Abstract 2576.
17. Isambert, N.; Campone, M.; Bourbouloux, E.; Drouin, M.; Major, A.; Yin, W.; Loadman, P.; Capizzi, R.; Grieshaber, C.; Fumoleau, P. *Eur. J. Cancer* **2009**, Dec 21, published on-line.
18. Nolan, K. A.; Doncaster, J. R.; Dunstan, M. S.; Scott, K. A.; Frenken, A. D.; Siegel, D.; Ross, D.; Barnes, J.; Levy, C.; Leys, D.; Whitehead, R. C.; Stratford, I. J.; Bryce, R. A. *J. Med. Chem.* **2009**, *52*, 7142.
19. Verdonk, M. L.; cole, J. C.; Hartshorn, M. J.; Murray, C. W.; Taylor, R. D. *Proteins* **2003**, *52*, 609.
20. Cheng, Y.; Prusoff, W. H. *Biochem. Pharmacol.* **1973**, *22*, 3099.
21. Stratford, I. J.; Stephens, M. A. *Int. J. Radiat. Oncol.* **1989**, *16*, 973.
22. Cholody, W. M.; Horowska, B.; Paradziej-Lukowicz, J.; Martelli, S.; Konopa, J. *J. Med. Chem.* **1996**, *39*, 1028.
23. Mazerska, Z.; Augustin, E.; Dziegielewski, J.; Cholody, M. W.; Konopa, J. *Anticancer Drug Des.* **1996**, *11*, 73.
24. De Marco, C.; Zaffaroni, N.; Comijn, E.; Tesei, A.; Zoli, W.; Peters, G. J. *Int. J. Oncol.* **2007**, *31*, 907.
25. Hyzy, M.; Bozko, P.; Konopa, J.; Skladanowski, A. *Biochem. Pharmacol.* **2005**, *69*, 801.
26. Rix, U.; Hantschel, O.; Dürnberger, G.; Remsing, R. L. L.; Planyavsky, M.; Fernbach, N. V.; Kaupe, I.; Bennett, K. L.; Valent, P.; Colinge, J.; Köcher, T.; Superti-Furga, G. *Blood* **2007**, *110*, 4055.
27. Lee, S. J.; Wang, J. Y. *J. Biol.* **2009**, *8*, 30.
28. Iskander, K.; Barrios, R. J.; Jaiswal, A. K. *Clin. Cancer Res.* **2009**, *15*, 1534.